

## Synthesis and Liposome Insertion of a New Poly(carboranylalkylthio)porphyrazine to Improve Potentiality in Multiple-Approach Cancer Therapy

Sandra Ristori,<sup>\*,†</sup> Anna Salvati,<sup>†</sup> Giacomo Martini,<sup>†</sup> Olivier Spalla,<sup>‡</sup> Daniela Pietrangeli,<sup>§</sup> Angela Rosa,<sup>§</sup> and Giampaolo Ricciardi<sup>§</sup>

Department of Chemistry, University of Firenze, Via della Lastruccia 3, 50019 Sesto Fiorentino (FI), Italy, DRECAM-SCM-LIONS, CEA Saclay, 91191 Gif Sur Yvette, France, and Department of Chemistry, University of Basilicata, Via N. Sauro 85, 85100 Potenza, Italy

Received August 24, 2006; E-mail: sandra.ristori@unifi.it

Porphyrins and related macrocycles are efficient sensitizers in anticancer treatments such as photodynamic therapy (PDT) and photothermal therapy (PTT).<sup>1–6</sup> Recently, these molecules have been derivatized with boron containing functions for possible use in boron neutron capture therapy (BNCT).<sup>3–5</sup> All of these therapies require a “bullet”, that is, light or neutrons, and an active compound, such as a strong neutron or light absorber, preferentially located inside malignant cells.<sup>6</sup> Here we describe a new poly(carboranylalkylthio)porphyrazine, (H<sub>2</sub>HECASPz, Figure 1), synthesized with the purpose to contribute to this issue. The choice of H<sub>2</sub>HECASPz was dictated by several factors. First, the notion that in the context of carboranyl-tetrapyrroles, polycarboranyl-alkylthio-porphyrazines represent an interesting variant, in that they conjugate high peripheral carboranyl substitution (80 boron atoms per macrocycle) with considerable flexibility of the azaporphyrin core and with the presence of eight electron rich sulfur atoms.<sup>7</sup> Second, the experimental evidence that this class of tetrapyrroles, depending on the peripheral substituents and the coordinated metal, may show intense absorbance in the “therapeutic window”, near-IR luminescence or rapid radiationless decay of the photogenerated S<sub>1</sub> (Q) state.<sup>1,2,6,8</sup> These properties make them well suited for anticancer multiple approach.

H<sub>2</sub>HECASPz was obtained by template cyclotetramerization of the 2,3 bis[6-(2-allyl-1,2-closo-dodecarboran-1-yl) hexylthio] maleonitrile over Mg(OPr)<sub>2</sub>, followed by mild demetallation with trifluoroacetic acid (see Supporting Information). H<sub>2</sub>HECASPz exhibits a strong Q-band at 712 nm ( $\epsilon = 2.8 \times 10^4 \text{ M}^{-1} \text{ cm}^{-1}$ ) and is not luminescent. So, we have a case of tetrapyrrole for which the S<sub>1</sub> (Q) state decays nonradiatively, even in the absence of a quenching coordinated metal.<sup>6,8</sup>

Vectors to deliver and concentrate the active molecules at target sites are extensively looked for and many delivery agents have been proposed, including surfactant-based structures,<sup>9</sup> polymers,<sup>10</sup> and, more recently, nanospheres<sup>11</sup> and nanotubes.<sup>12</sup> However, only liposomes are currently accepted for clinical tests on humans.<sup>13</sup> Here we loaded liposomes with H<sub>2</sub>HECASPz. The loaded vectors were characterized by dynamic light scattering (DLS), zeta potential ( $\zeta$ ), and synchrotron small-angle X-ray scattering (SAXS). Valuable information on the host–guest interactions at the molecular level were obtained by density functional theory (DFT) calculations.

As liposome constituents, we used 1,2-dioleoyl-*sn*-glycero-phosphocholine (DOPC) and 1,2-dioleoyl-*sn*-glycero-phospho-ethanolamine (DOPE). PC and PE polar heads are the most abundant in plasma membranes and are known to be compatible with cells. Long and flexible dioleoyl chains were required to accommodate the bulky H<sub>2</sub>HECASPz molecule (~40 Å in its

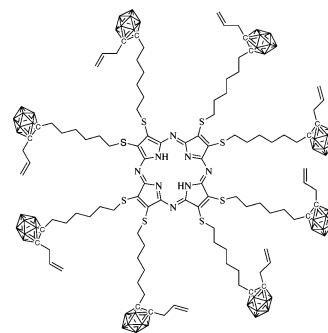


**Figure 1.** Molecular structure of H<sub>2</sub>HECASPz.

extended form). Liposomes were prepared by two different methods, that is, detergent depletion with sodium cholate, and extrusion. Typical SAXS curves at the absolute scale are reported in Figure 2. Plain and porphyrazine loaded liposomes prepared by detergent depletion (Figure 2A) showed  $I(q)$  versus  $q$  diagram characteristic of monolamellar liposomes, which could be fitted by using the form factor of a bilayer:

$$I(q) = \frac{4\pi}{q^4} \Sigma \left[ (\rho_c - \rho_h) \sin\left(\frac{q t_c}{2}\right) + (\rho_h - \rho_s) \sin\left(\frac{2t_h + t_c}{2} q\right) \right]^2 \quad (1)$$

where  $\rho_c$ ,  $\rho_h$ ,  $t_c$ , and  $t_h$  are the electronic density and the thickness of the hydrophobic and hydrophilic layer, respectively,  $\rho_s$  is the electronic density of the solvent, and  $\Sigma$  is the interface extension per unit volume. A Gaussian distribution of  $t_c$  (with half-height width  $\delta t_c$ ) was allowed to blur out the sharp minima in eq. 1 and to take into account a small degree of polydispersity. The relevant parameters extracted from the fitting are reported in Table 1 together with the aggregate mean diameter ( $D$ ), size polydispersity, and  $\zeta$ -potential, which is directly related to the total surface charge. All these physical properties showed that progressive insertion of H<sub>2</sub>HECASPz slightly affected the host liposomes, but did not disrupt their basic structure nor modified their monolamellar nature. In particular, the electronic density decreased in the hydrophobic core and increased in the hydrophilic layer. This meant that less polar and/or smaller units were intercalated among the lipid chains, whereas association occurred between the polar heads and electron rich units.

The SAXS diagrams of liposomes prepared by extrusion (Figure 2B) showed correlation peaks due to interactions among lipid bilayers. Therefore, oligolamellar aggregates were formed, and Bragg peaks at  $q$  spacing 1:2:3 became more evident with increasing H<sub>2</sub>HECASPz content. This was probably favored by the well-known tendency of porphyrin-like rings to interact with each other and build stacking structures.<sup>2</sup> DLS measurements did not show any definite trend in this case (see Supporting Information).

<sup>†</sup> University of Firenze.

<sup>‡</sup> CEA Saclay.

<sup>§</sup> University of Basilicata.

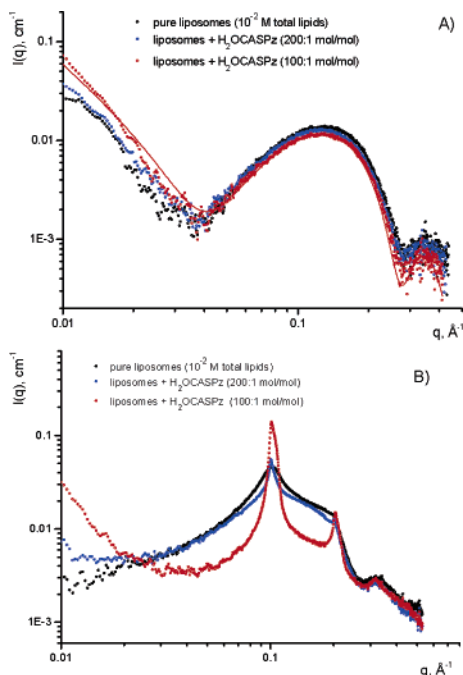


**Figure 2.** SAXS diagrams of plain and porphyrazine loaded DOPC/DOPE 1/1 liposomes prepared by detergent depletion (2A) and by extrusion (2B). The same H<sub>2</sub>HECASPz/lipid starting ratios were used for the two preparation methods, as indicated in the legend. Spectrophotometric quantitative analysis showed that 6–10% loading was obtained by extrusion and 38–55% by detergent depletion (see Supporting Information). The curves in panel A were fitted with eq 1, as stated in the text. For clarity, only the simulated curve of the liposomes + H<sub>2</sub>HECASPz 200:1 system has been reported (continuous red line).

**Table 1.** Best Fit Parameters for SAXS Curves of Liposomes Prepared by Detergent Depletion. The Initial Lipid/H<sub>2</sub>HECASPz Molar Ratios Are Indicated for Loaded Liposomes

| system                       | liposomes                        | liposomes + H <sub>2</sub> HECASPz (200:1) | liposomes + H <sub>2</sub> HECASPz (100:1) |
|------------------------------|----------------------------------|--|--|
| $\rho_c$ (cm <sup>-2</sup> ) | $(7.8 \pm 0.1) \times 10^{10}$   | $(6.6 \pm 0.1) \times 10^{10}$             | $(6.0 \pm 0.1) \times 10^{10}$             |
| $\rho_h$ (cm <sup>-2</sup> ) | $(1.32 \pm 0.01) \times 10^{11}$ | $(1.41 \pm 0.01) \times 10^{11}$           | $(1.46 \pm 0.01) \times 10^{11}$           |
| $t_c$ (Å)                    | 26.4                             | 25.3                                       | 24.8                                       |
| $\delta t_c$                 | 2.3                              | 2.8  | 3  |
| $t_h$ (Å)                    | $5.7 \pm 0.1$                    | $8.2 \pm 0.1$                              | $9.1 \pm 0.1$                              |
| $D$ (nm)                     | $134 \pm 5$                      | $200 \pm 10$                               | $190 \pm 15$                               |
| polyd                        | 0.26                             | 0.31                                       | 0.38                                       |
| $\zeta$ (mV)                 | $-11 \pm 3$                      | $-8 \pm 2$                                 | $-6 \pm 2$                                 |

Interestingly, insertion of H<sub>2</sub>HECASPz into liposomes was accompanied by marked hypochromism of the porphyrazine Q-band and by the appearance of an “extra” band at 585 nm (see Supporting Information). The above-mentioned structural and spectroscopic variations suggested that, besides substantially aspecific intermolecular forces, localized host–guest interactions could be crucial in driving the supramolecular architecture. To confirm this hypothesis we turned to density functional theory (DFT) calculations. Unconstrained geometry optimization at the BP86/TZ2P level of the {H<sub>2</sub>OMSPz[NH<sub>3</sub>(CH<sub>2</sub>)<sub>2</sub>HPO<sub>4</sub>]} model complex obtained by replacing the peripheral tails with methyl groups, gave the stable C<sub>1</sub> symmetry structure displayed in Figure 3. In this complex, nearly linear hydrogen bonds bridge a pyrrole N<sub>p</sub>H proton to one oxygen atom of the phosphate group and a NH proton of the PE head to a porphyrazine aza-methyne, N<sub>b</sub>. The N<sub>p</sub>⋯O and N<sub>b</sub>⋯N<sub>PE</sub> distances (2.674 Å and 2.739 Å, respectively) fit in with experimental and theoretical data reported for similar structures.<sup>14</sup> Hydrogen-bond formation enhances the distortion of the porphyrazine core, and the involved pyrrole ring is tilted 23.5° and 17.8° from the adjacent pyrrole planes. The energy required for this distortion amounts to

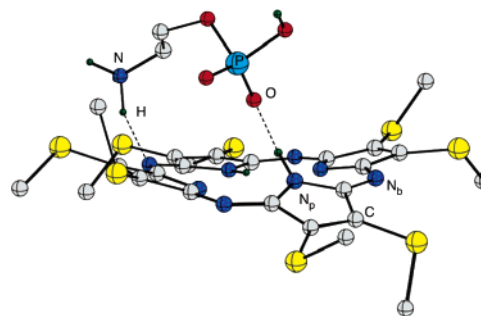


**Figure 3.** DFT optimized structure of the model complex {H<sub>2</sub>OMSPz-[NH<sub>3</sub>(CH<sub>2</sub>)<sub>2</sub>HPO<sub>4</sub>]}. For clarity, the hydrogen atoms of the porphyrazine sulfanylmethyl groups are omitted.

~13 kcal mol<sup>-1</sup> and is paid back by the hydrogen-bond interactions, which are exothermic by 40.6 kcal mol<sup>-1</sup>. The changes in the porphyrazine optical spectrum induced by supramolecular interactions were well reproduced by time dependent-DFT (TDDFT) calculations. Indeed, a 70% reduction of the oscillator strength is predicted for the Q-band, and a new absorption with oscillator strength of 0.107 is computed at 593 nm.

In summary, experimental and theoretical data showed that effective interactions set up between the newly synthesized polycarboranyl porphyrazine and the polar heads of liposome constituents, indicating a useful strategy for the design of new tetrapyrrolic systems to be loaded in liposomes and delivered through the membrane of cancerous tissues. This is a favorable starting point for anticancer multiple-approach therapy.

**Acknowledgment.** Thanks are owed to the Italian Consorzio Interuniversitario per lo Sviluppo dei Sistemi a Grande Interfase (CSGI) and to the Ministero dell’Istruzione, dell’Università e della Ricerca (MIUR) for financial support. The European Synchrotron Radiation Facility (ESRF) is kindly acknowledged for beam time allocation.

**Supporting Information Available:** Synthetic and computational details, liposome preparation and characterization, electronic spectra of H<sub>2</sub>HECASPz loaded in liposomes. This material is available free of charge via the Internet at <http://pubs.acs.org>.

## References

- (1) (a) Montalbano, A. G.; Baum, S. M.; Barrett, A. G. M.; Hoffman, B. M. *Dalton Trans.* **2003**, 2093–2102. (b) Hammer, N. D.; Vesper, B. J.; Elseth, K. M.; Hoffman, B. M.; Barrett, A. G. M. *J. Med. Chem.* **2005**, *48*, 8125–8133.
- (2) Donzello, M. P.; Ercolani, C.; Stuzhin, P. A. *Coord. Chem. Rev.* **2006**, *250*, 1530–1561.
- (3) Luguya, R. J.; Fronczek, F. R.; Smith, K. M.; Vicente, M. G. H. *Tetrahedron Lett.* **2005**, *46*, 5365–5368.
- (4) Gottumukkala, V.; Luguya, R. J.; Fronczek, F. R.; Vicente, M. G. H. *Bioorg. Med. Chem.* **2005**, *13*, 1633–1640.
- (5) Wu, H.; Micca, P. L.; Makar, M. S.; Miura, M. *Bioorg. Med. Chem.* **2006**, *14*, 5083–5092.
- (6) Szacilowski, K.; Macyk, W.; Drzewiecka-Matuszek, A.; Brindell, M.; Stochel, G. *Chem. Rev.* **2005**, *105*, 2647–2699.
- (7) (a) Ricciardi, G.; Rosa, A.; Ciofini, I.; Bencini, A. *Inorg. Chem.* **1999**, *38*, 1422–1431. (b) Ricciardi, G.; Belviso, S.; Giancane, G.; Tafuro, R.; Wagner, T.; Valli, L. *J. Phys. Chem. B* **2004**, *108*, 7854–7861.
- (8) Gunaratne, T. C.; Gusev, A. V.; Peng, X.; Rosa, A.; Ricciardi, G.; Baerends, E. J.; Rizzoli, C.; Kenney, M. E.; Rodgers, M. A. *J. Phys. Chem. A* **2005**, *109*, 2078. (b) Ricciardi, G.; Soldatova, A. V.; Rodgers, M. A. J. Unpublished work.
- (9) Drummond, C. J.; Fong, C. *Curr. Opin. Colloid Interface Sci.* **1999**, *4*, 449–456.
- (10) Chasin, M.; Langer, R., Eds. *Drugs and the Pharmaceutical Sciences*; Marcel Dekker: New York, 1990; Vol. 45.
- (11) Labhasetwar, V.; Song, C.; Levy, R. *J. Adv. Drug. Del. Rev.* **1997**, *24*, 63–85.
- (12) Yinghuai, Z.; Peng, A. T.; Carpenter, K.; Maguire, J. A.; Hosmane, N. S.; Takagaki, M. *J. Am. Chem. Soc.* **2005**, *127*, 9875–9880.
- (13) Torchilin, V. P. *Nat. Rev. Drug Discovery* **2005**, *4*, 145–160.
- (14) (a) Gilli, P.; Bertolasi, V.; Pretto, L.; Antonov, L.; Gilli, G. *J. Am. Chem. Soc.* **2005**, *127*, 4943–4953. (b) Estrada, E.; Simon-Manso, Y. *Angew. Chem., Int. Ed.* **2006**, *45*, 1719–1721.

JA0661459